Ground Penetrating Radar
The first peer-reviewed scientific journal dedicated to GPR

GROUND PENETRATING RADAR INVESTIGATIONS IN SITES OF CULTURAL INTEREST IN MALTA

RAFFAELE PERSICO[1], SEBASTIANO D'AMICO[2], ENZO RIZZO[3], LUIGI CAPOZZOLI[3] & AARON MICALLEF[2]

[1] INSTITUTE FOR ARCHAEOLOGICAL AND MONUMENTAL HERITAGE OF THE NATIONAL RESEARCH COUNCIL (IBAM-CNR), LECCE, ITALY
R.PERSICO@IBAM.CNR.IT

[2] UNIVERSITY OF MALTA, FACULTY OF SCIENCE, MSIDA, MALTA
SEBASTIANO.DAMICO@UM.EDU.MT, AARON.MICALLEF@UM.EDU.MT

[3] INSTITUTE OF METHODOLOGIES FOR ENVIRONMENTAL ANALYSIS OF THE NATIONAL RESEARCH COUNCIL (CNR-IMAA), TITO SCALO – POTENZA, ITALY
ENZO.RIZZO@IMAA.CNR.IT, LUIGI.CAPOZZOLI@IMAA.CNR.IT

ABSTRACT

This paper presents the results of a series of geophysical surveys carried out in Malta. In particular, we used a reconfigurable stepped-frequency Ground Penetrating Radar (GPR) prototype to inspect the Argotti Garden in Floriana, looking for ancient buried cisterns, and the floor of the Nymphaeum inside the garden, to assess its conditions prior to restoration works. We subsequently used a commercial pulsed GPR system to assess the walls of the co-cathedral of St. John, in Valletta, and the walls of a building of the University of Malta, in Msida. All measurements were performed during a Short-Term Scientific Mission (STSM) funded by the COST (European Cooperation in Science and Technology) Action TU1208 "Civil engineering applications of Ground Penetrating Radar." Of course the work performed during the STSM consisted also in the processing and interpretation of the gathered data.

KEYWORDS: Ground Penetrating Radar; Cultural heritage; Detection of buried structures; Inspection of walls; Estimation of propagation velocity and relative permittivity.

1. INTRODUCTION

A Short-Term Scientific-Mission (STMS) entitled "Integrated geophysical investigations of sites of cultural interest in Malta" was recently funded by COST (European Cooperation in Science and Technology), in the framework of the COST Action TU1208 "Civil engineering applications of

https://doi.org/10.26376/GPR2018002

Ground Penetrating Radar." Raffaele Persico, Luigi Capozzoli and Enzo Rizzo visited Sebastiano D'Amico and Aaron Micallef in Malta, from March 5th to March 18th, 2017, and they jointly investigated a series of sites of cultural interest.

The initial plan was to survey the following archaeological and historical sites: the Argotti Botanical Garden in Floriana and the Nymphaeum inside the garden, the co-cathedral of St. John in Valletta, and the Palace de la Salle, still in Valletta. In the latter site, the degradation of frescoes did not allow performing the scheduled investigations. Some results obtained in the co-cathedral of St John, where a few walls were investigated, looked rather obscure and difficult to be interpreted; for comparison purposes, further tests were performed on similar walls in the University of Malta, in Msida. The walls of the co-cathedral and those of the university building were both nominally made of globigerina. Therefore, although we could not perform the planned measurements in the Palace de la Salle, we dealt with the inspection of the walls in the university, which was not initially scheduled, and the total number of case studies did not change. In this paper, all results obtained during the STSM are presented. The work performed during the STSM consisted also in the processing of the recorded data and their interpretation.

In the Argotti Botanical Garden (Section 2), four Ground Penetrating Radar (GPR) profiles (B-Scans) were collected by using a stepped-frequency reconfigurable GPR prototype. Additionally, we processed and interpreted some data previously gathered in the same garden, by a different team, by using a commercial pulsed GPR system. In the Nymphaeum and its surroundings (Section 3), a grid of short GPR profiles was acquired by using the stepped-frequency reconfigurable GPR prototype.

We collected five GPR profiles on the walls of the co-cathedral of St. John in Valletta (Section 4) and sixteen GPR profiles on the walls of the University of Malta, in Msida (Section 5).

2. The Argotti Botanical Garden in Floriana

The Argotti Botanical Garden of Malta has an historical relevance. It is found in an area where the Knives constructed large cisterns for gathering the water for the needs of the island (in particular for Valletta

https://doi.org/10.26376/GPR2018002

and for the settlements around Valletta). Some of these cisterns are visible and we have seen one of them in the Botanical Garden; it is deemed that other cisterns are present in the garden. The cisterns are expected to expand at a depth of 5 to 6 meters, where they become hundredths cube meter large, as big demijohns. In order to identify them, we exploited a stepped frequency reconfigurable ground penetrating radar, initially designed and realized within the project AITECH (http://www.aitechnet.com/ibam.html), funded by the Puglia Region, and more recently improved in the framework of the COST Action TU1208. We gathered four B-Scans in the Botanical Gardens, looking for the cisterns, as shown in Figure 1.

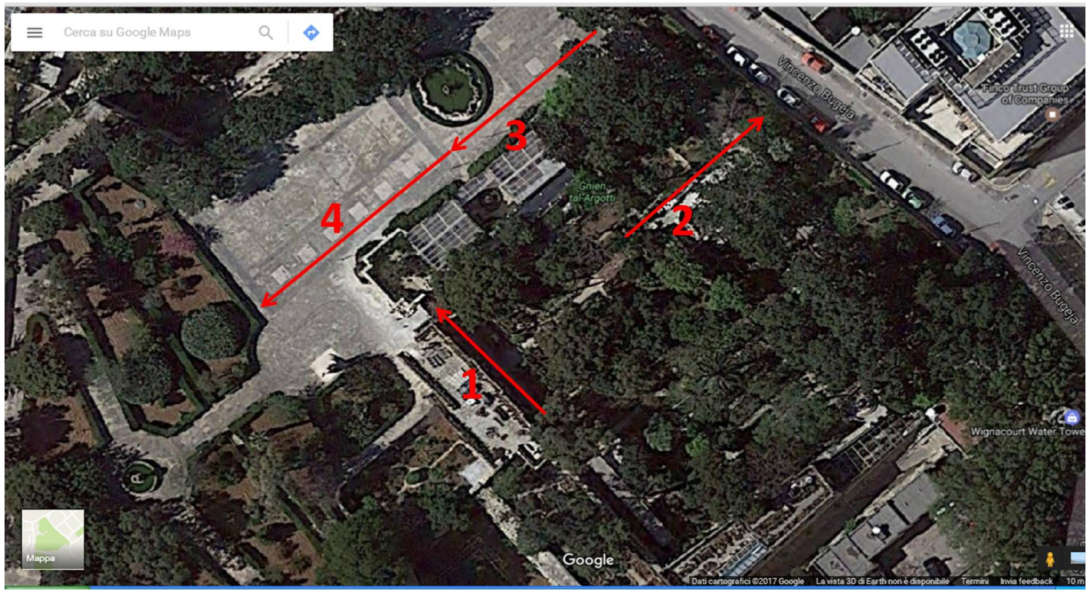

FIG. 1 - Map of the B-Scans gathered in the Argotti Garden.

The B-Scans were labelled as BScan1, BScan2, BScan3 and BScan4. The presence of plants in the garden prevented from prospecting more completely the area. To be precise, BScan3 and BScan4 were gathered outside the garden, where a large area was available; unfortunately we did not have the permissions for acquiring more data and for prospecting the entire area.

As a preliminary step, we repeated BScan1 twice, in order to check whether there was a meaningful electromagnetic interference. This task was possible thanks to some advanced features recently implemented in

https://doi.org/10.26376/GPR2018002

the reconfigurable GPR. We do not describe in detail the exploited algorithm, because this was developed during a previous STSM: for more information please see [1-3]. Here, we just wish to say that the data showed no significant interference problems in the cases at hand.

All data presented in Figures 2-4 were recorded by the low frequency antennas of the reconfigurable GPR, with a central frequency of about 120 MHz: the targets of interest, in the case at hand, were large and possibly quite deep; therefore, this band was the most promising one.

The data processing included: zero timing, background removal, gain application versus depth, a slight one-dimensional filtering, and visualization of the first 50 ns of the signal. Then, the data were migrated.

The most interesting anomalies in Figures 2 to 5 are circled in red. We did not identify clear traces of possible buried cisterns.

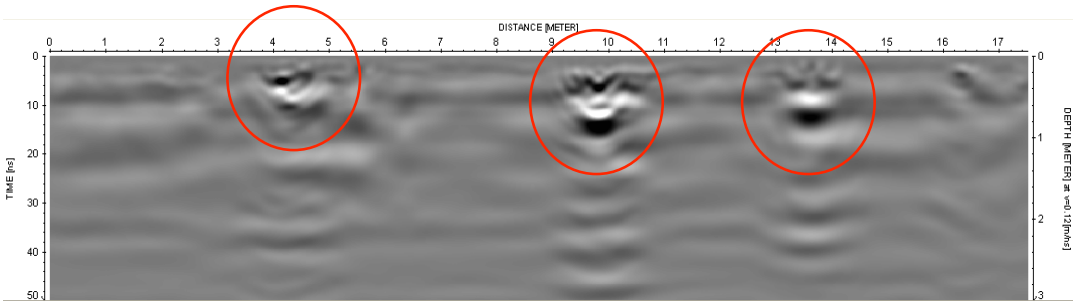

FIG. 2 - Elaboration of BScan1.

What a GPR can probably see is the upper part of a cistern, closer to the mouth, or closer to a point that used to be the mouth. Anomalies ascribable to cisterns would probably appear rather small, compared to the cistern size. This is because the bottom of the cistern is too far and consequently the radiated energy is lost in scattering phenomena. Moreover, we cannot exclude the possibility that some cisterns could be partially filled up with loose materials. In that case, we would not have a buried empty cavity as large as the cistern used to be at the time of the Knives.

Further to gather our own data, we had at our disposal some data previously gathered by a local company by using a commercial GPR system manufactured by MALÅ equipped with a 150 MHz antenna. We did not have more information about their data. In particular, we did

https://doi.org/10.26376/GPR2018002

not know the precise localization of the B-Scans, although we knew that they were collected in the same area as our B-Scans 3 and 4 (Figure 1). The processing of the data was similar to that preformed for our data, with some different specific data (and antenna) driven parameters. The results are presented in Figures 6 to 9.

Also in the data collected by the company, a direct evidence of the cisterns cannot be found. Some superficial anomalies are hardly visible, indicated by red arrows. It is evident that a strong phenomenon of antenna ringing occurred and the quality of the images is lower.

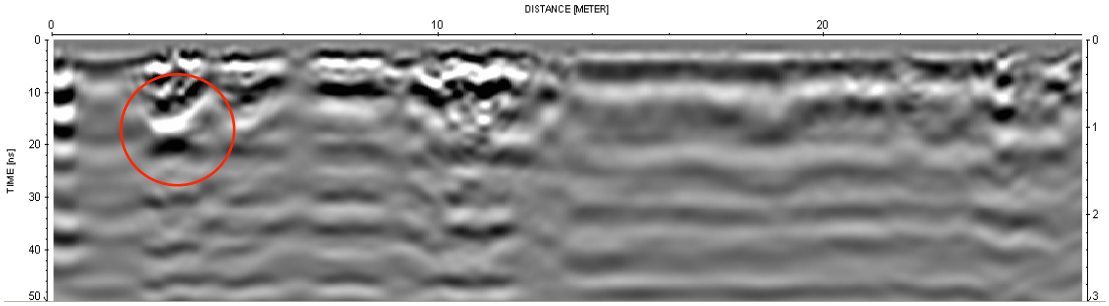

FIG. 3 - Elaboration of BScan2.

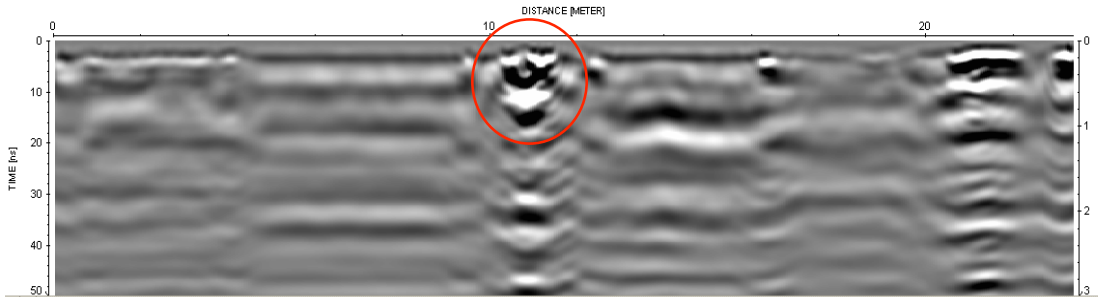

FIG. 4 - Elaboration of BScan3.

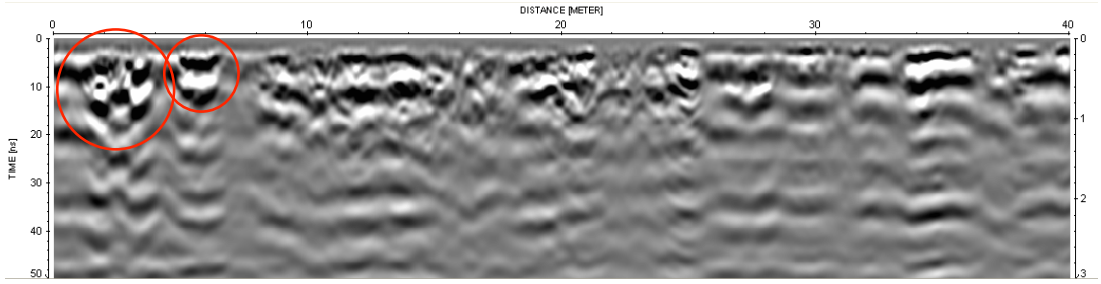

FIG. 5 - Elaboration of BScan4.

https://doi.org/10.26376/GPR2018002

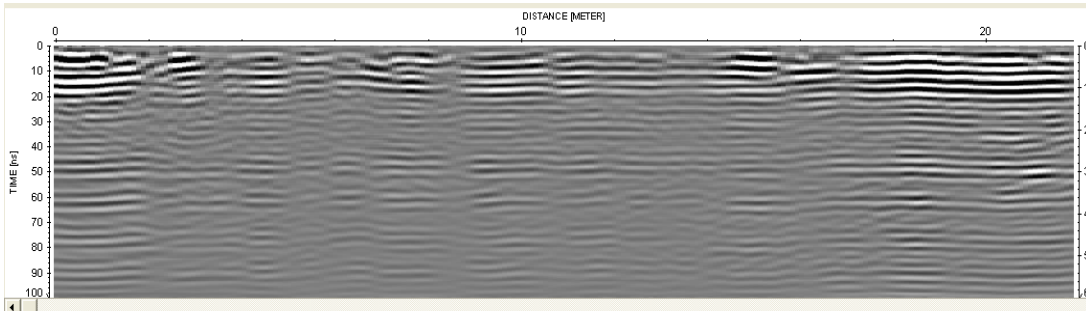

FIG. 6 - First B-Scan gathered with a commercial system.

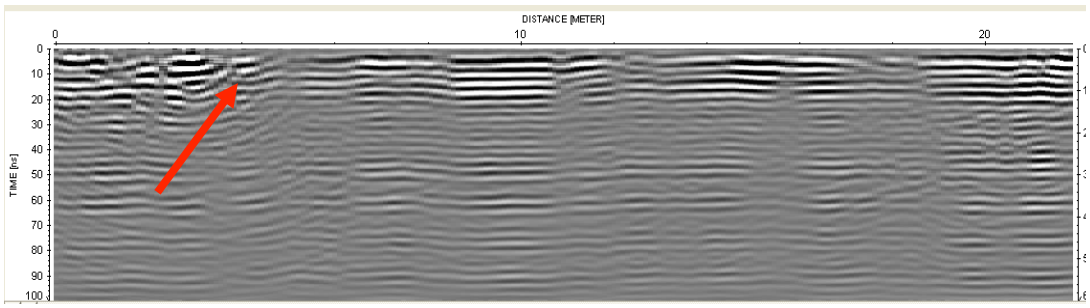

FIG. 7 - Second B-Scan gathered with a commercial system.

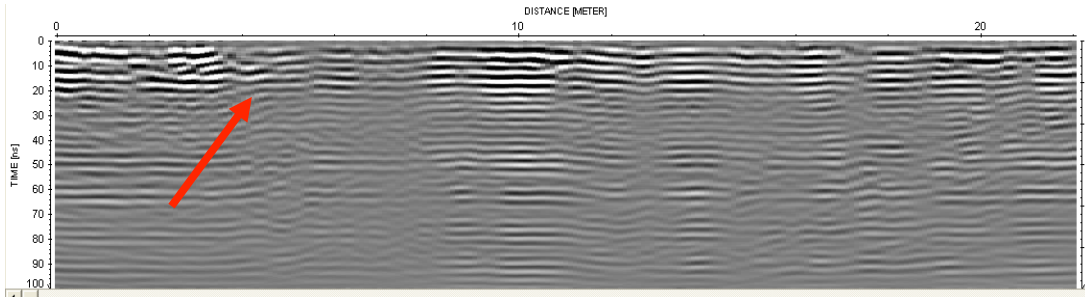

FIG. 8 - Third B-Scan gathered with a commercial system.

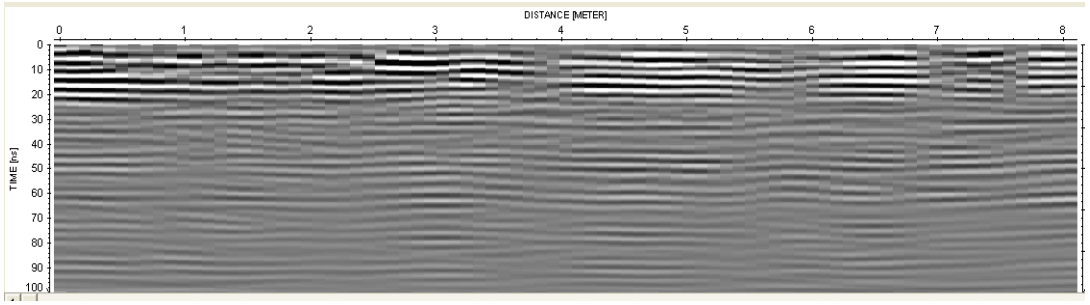

FIG. 9 - Fourth B-Scan gathered with a commercial system.

https://doi.org/10.26376/GPR2018002

The problem of finding the cisterns is of interest for the local cultural authorities. As a conclusion of our preliminary study, we communicated them that an integrated prospecting could help to achieve more information about the subsurface and the presence of cisterns. In particular, permission for gathering a sufficient number of GPR profiles in the area adjacent to the gardens is necessary, in particular we need to acquire a grid of profiles in order to realize horizontal images of the ground, at different depths (slices). This will help to discriminate if some anomalies can be ascribable to the top of cisterns. Moreover, and above all, a three dimensional geoelectrical prospecting would be more suitable for this kind of investigation than a GPR survey, given the depth and strong resistivity of the anomalies looked for (if big cavities were present). Last but not least, the geoelectrical prospecting should be slightly invasive, in the sense that the electrodes should be knocked beyond the asphalt layer, which therefore should be removed in some (very small) regions and then restored after the investigation. Non-invasive electrodes exist, which can be placed over the surface, however in this case they would not work because the asphalt is electrically insulating.

3. The Nymphaeum of the Argotti Botanical Garden in Floriana

Within the Argotti Garden there is a Nymphaeum of artistic and historical relevance. Nowadays, it is not perfectly preserved and needs restoration works. In order to perform in a safe way such works, and in particular in order to put the scaffoldings in a non-dangerous way (for the possible presence of cavities under the floor), it was of interest to perform a GPR prospecting. So, we gathered a grid of profiles within the Nymphaeum, by using our reconfigurable stepped-frequency GPR system. We also prospected part of the path that brings to the Nymphaeum. As the signal returned by the two areas was quite different, two different processing procedures were applied, in order to emphasize the internal and external anomalies.

The first processing, for data gathered inside the Nymphaeum, was composed by zero timing at 0.8 ns, background removal on all the traces, gain function with linear amplification factor equal to 1, exponential amplification factor equal to 2, and saturation at 10000. Then, a background filtering followed, with moving averaging on 26

https://doi.org/10.26376/GPR2018002

traces. Finally, a Kirchhoff migration on 25 traces with a propagation velocity of 0.12 m/ns was performed.

After the processing, horizontal slices were retrieved. The profile spacing was 20 cm and high frequency antennas were used (their band overall covers the 500 MHz to 1000 MHz range), because this time we were looking for shallower and smaller targets. In Figures 10 to 14, some slices are shown relative to this processing, aimed to emphasize the anomalies below the floor of the Nymphaeum; the GPR data are superimposed to the map of the Nymphaeum (axes are in meters).

The more superficial slices tell us that the main anomalies are located in the part of the Nymphaeum closer to the entrance. Those anomalies might be due to previous foundations, else to a different composition or density of the subsoil. From the data, we excluded the presence of superficial cavities.

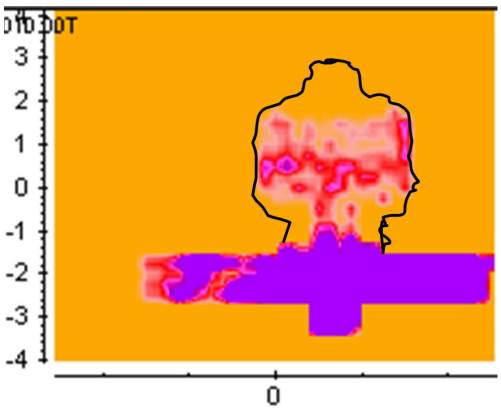

FIG. 10 - Slice at about 12 cm depth.

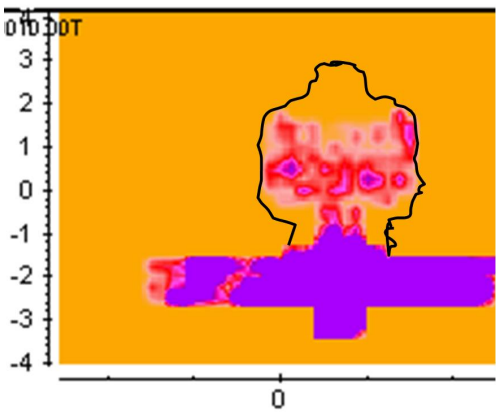

FIG. 11 - Slice at about 24 cm depth.

https://doi.org/10.26376/GPR2018002

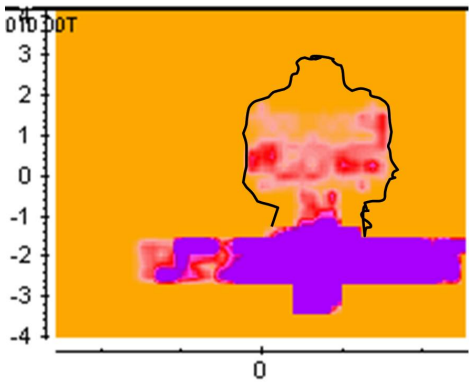

FIG. 12 - Slice at about 36 cm depth.

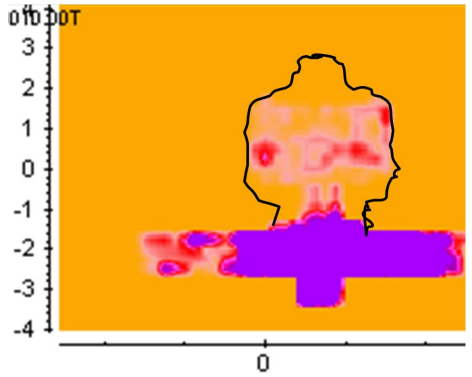

FIG. 13 - Slice at about 48 cm depth.

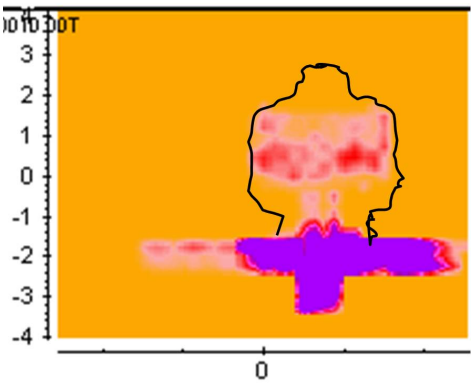

FIG. 14 - Slice at about 60 cm depth.

We tried a slightly different processing, to better emphasize the anomalies outside the Nymphaeum. The new processing was composed by a time cut at 70 ns, zero timing at -8 ns, background with running averaging on 51 traces, a gain function with parameters 1 and 1 for the linear and exponential amplification respectively, and with saturation at

https://doi.org/10.26376/GPR2018002

10000. Then a Butterworth filter in the band 50-1000 MHz was applied and finally a Kirchoff migration on 17 traces with propagation velocity estimated equal to 0.09 m/ns. The results are presented in the slices of Figures 15 to 17.

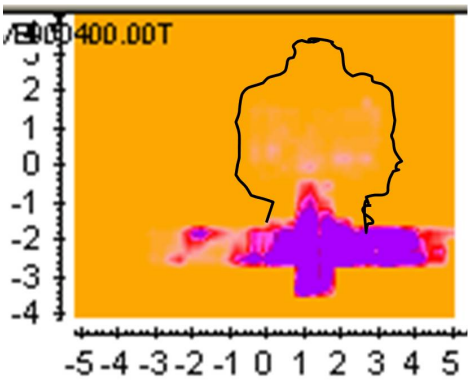

FIG. 15 - Slice at about 18 cm - second processing procedure.

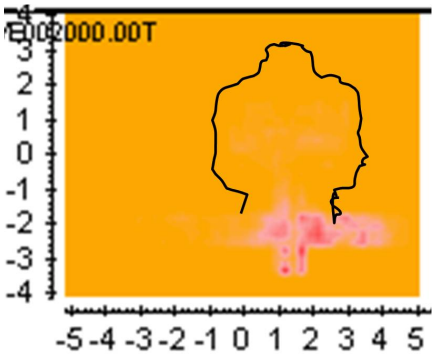

FIG. 16 - Slice at about 90 cm - second processing procedure.

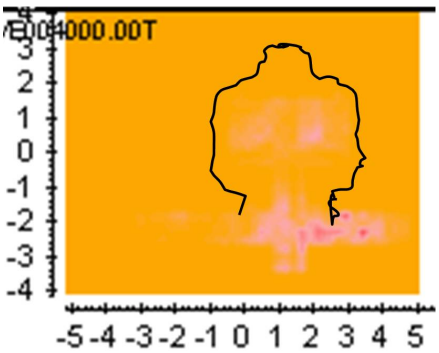

FIG. 17 - Slice at about 180 cm - second processing procedure.

https://doi.org/10.26376/GPR2018002

Outside the Nymphaeum we did not identify any meaningful buried anomaly, we just observed very different reflection characteristics before the Nymphaeum and immediately after the entrance of the Nymphaeum. This suggests that the concrete path is made of different materials than the concrete floor in the Nymphaeum; quite probably it was realized in a different period. Alternatively, some works interested in the past only part of the path, thus causing the different electromagnetic response.

4. WALLS OF THE CO-CATHEDRAL OF ST. JOHN IN VALLETTA

The co-cathedral of St. John is one of the most important monuments in Malta. This is the cathedral were the Grand Masters of Knives used to be buried. It is a masterpiece of Baroque style and hosts important frescoes, floor mosaics and paintings. Our objective was to investigate whether it was possible to retrieve some physical properties of the walls of the cathedral and detect possible internal fractures, meaningful gradients of moisture, or even possible structures inside the walls, hidden and walled during the past centuries.

In this case we made use of a commercial pulsed GPR system, RIS HI Mode manufactured by IDS Ingegneria dei Sistemi, equipped with a 2000 MHz nominal central frequency antenna.

The first pursued goal was to evaluate the relative dielectric permittivity of the walls. The relative permittivity ε_r of a wall built with a non-magnetic material can be easily calculated from GPR data as follows. If p is the thickness of the wall and t is the instant when the echo coming from the other side of the wall is observed (with respect to the side where we put the antenna on the wall), then the propagation velocity c of the electromagnetic waves in the wall can be estimated as:

$$c = 2p/t \tag{1}$$

where the presence of the factor 2 is due to the fact that the radiated pulse has to reach the other side of the wall and back-propagate to the GPR antenna. Implicit assumptions to use this formula are: the frequency dispersion is neglected, the electromagnetic wave is assumed to be substantially 'TEM' (transverse electromagnetic) with respect to the air-wall interface, and the wall is assumed to be composed of a homogeneous material. As we are assuming that the wall material is nonmagnetic, the propagation velocity of the waves in the wall is linked

https://doi.org/10.26376/GPR2018002

to the propagation velocity of the waves in air ($c_0 = 3\ 10^8$ m/s) by the well-known relationship:

$$c = c_0/\sqrt{\varepsilon_r} \tag{2}$$

By exploiting (1) and (2), it is easy to obtain:

$$\varepsilon_r = \left(\frac{tc_0}{2p}\right)^2 \tag{3}$$

where t was measured with a GPR and p was measured with a common tape meter.

It may happen that the other side of the wall is not visible, e.g., because the wall is too thick and the losses too intense. It may also happen the wall is stratified and in this case it is not immediate to recognize, among several flat reflectors identifiable in the signal, which one can be ascribed to the other side of the wall. A metal sheet put on the other side of the wall can be useful to enhance the relevant reflection.

When the other side of the wall is not visible, the propagation velocity in the wall can be estimated from the diffraction hyperbolas visible in the data, if any. In particular, if a target is small with respect to the central wavelength of the emitted pulse, then, at a position x, the return time t of the pulse reflected by a target is linked to the propagation velocity c by the following equation:

$$t = \frac{2}{c}\sqrt{(x - x_0)^2 + \left(\frac{ct_0}{2}\right)^2} \tag{4}$$

where x_o is the abscissa of the axis of the small target and t_o is the minimum return time, measured when the GPR passes over the target. Equation 4 describes a hyperbola in the plane (x, t). The hyperbola is parametric in c and can be graphically matched with a trial hyperbola having the same vertex (x_o, t_o) and larger or narrower prongs depending on the chosen trial value of c. More details about this procedure can be found in the literature [4].

Coming back to our investigations in the co-cathedral of St. John, we performed a measurement on the wall of the chapel of the Oratory. The wall was quite thick: the other accessible side was about 5 meters distant. It was therefore difficult to see the other side of the wall with the antenna at disposal; we hoped to find some non-homogeneities in the wall, which would have permitted us to apply the hyperbola

https://doi.org/10.26376/GPR2018002

procedure described above and estimate an average value of the relative permittivity in the medium at hand. But, the results presented in Figure 18 show revealed that the wall is very homogeneous, therefore we could not perform any permittivity evaluation.

After a processing composed by zero timing at 4 ns, background removal, gain application versus depth and Butterworth filtering in the band 50 MHz - 3500 MHz, we observed that the signal just sank progressively in the noise versus the depth. No meaningful internal fracture, no meaningful gradient of moisture and no walled feature were detected. The scan of the wall was performed from the floor level up, and we just identified some flat reflection in the lower part, maybe due to the plaster.

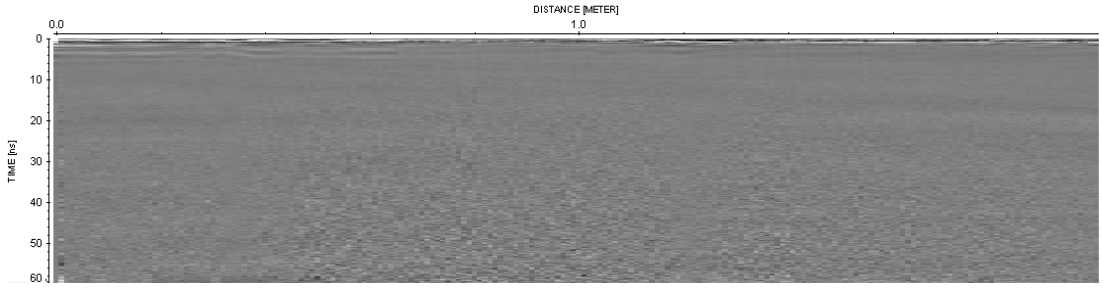

FIG. 18 - Processed B-Scan gathered on the wall of the chapel of the oratory.

Then, we prospected another wall, which was only 25 cm thick, in a corridor of the Oratory. We repeated the measurements twice, the second time putting a flat metal (copper) sheet on the other side of the wall, in order to carry out a comparison of the reflections achieved with and without the metal sheet. The length of the metal sheet was about 1 m, its width was about 50 cm and its thickness was 5 mm. The reflection from the metal sheet, if visible, would enable to estimate the propagation velocity of the electromagnetic waves in the wall (and we might assume the same propagation velocity in all the walls of the cathedral, although we do not know whether they are all made with the same material). The results are shown in Figure 19. The B-Scans were gathered in the bottom up direction, starting from the floor level. Unfortunately, the other side of the wall was not visible, which this time was absolutely not expected. This means that the walls of the cathedral are highly lossy. Moreover, also in this case the wall appears to be rather homogeneous.

https://doi.org/10.26376/GPR2018002

The processing procedure was similar to the previous case, with just some small data driven difference. This holds also with regard to the next B-Scans that we are going to show.

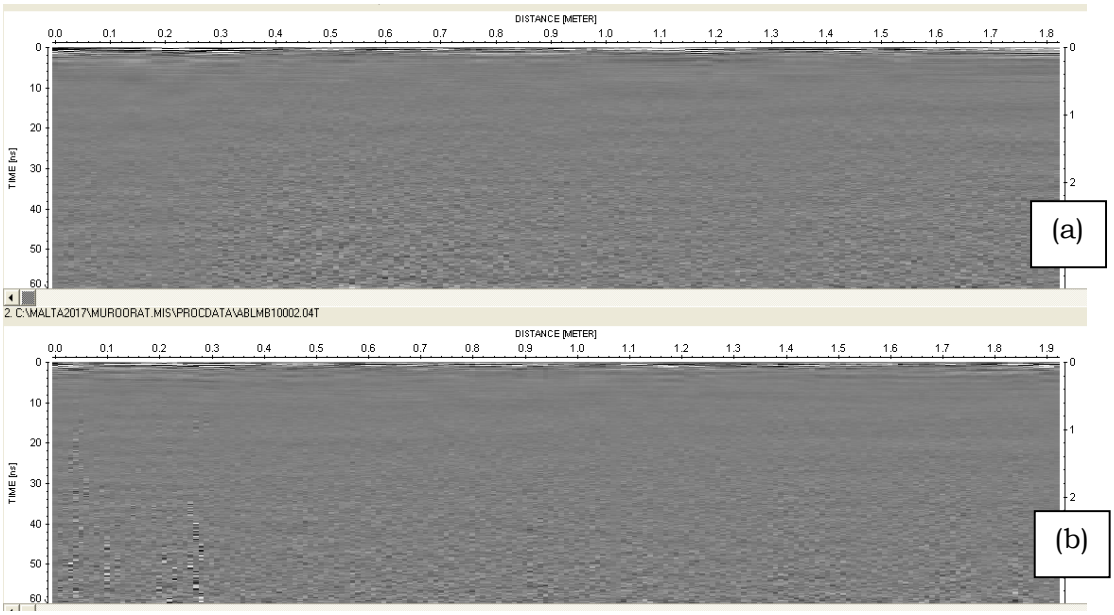

FIG. 19 - (a) B-Scan gathered on a 25-cm thick wall, in the co-cathedral of St. John and (b) B-Scan gathered on the same wall, with a metallic sheet on the opposite side of the wall.

We continued our investigation in the co-cathedral and found an ashlar along the stairs that lead to the "Bartolotti Chapel," probably of the same kind of the ashlar exploited for restoring works. Incidentally, the Bartolotti chapel was below the Oratory and was closed to the public. We repeated our measurements on the ashlar twice, the second time placing the copper sheet behind the ashlar; results are presented in Figure 20. The signal was not very clear, because the reduced size of the ashlar caused the presence of multiple reflections coming from several directions, which amplitudes were much higher than in the previous cases. Nonetheless, this time the effect of the copper sheet was visible in the radargram and we have indicated it with a black arrow in Figure 20(b): the copper sheet made the reflection from the other side of the ashlar stronger and masked the deeper echoes. The reflection does not look perfectly parallel to the air-ashlar interface, because the shape of the external surface of the ashlar was not perfectly flat. As the reflection

https://doi.org/10.26376/GPR2018002

coming from the other side appeared to be at about 6 ns, we estimated a velocity of propagation of 6 cm/ns. This means that the relative permittivity is approximately equal to 25: such value is compatible with the humid environment, which makes humid (and lossy) the stones.

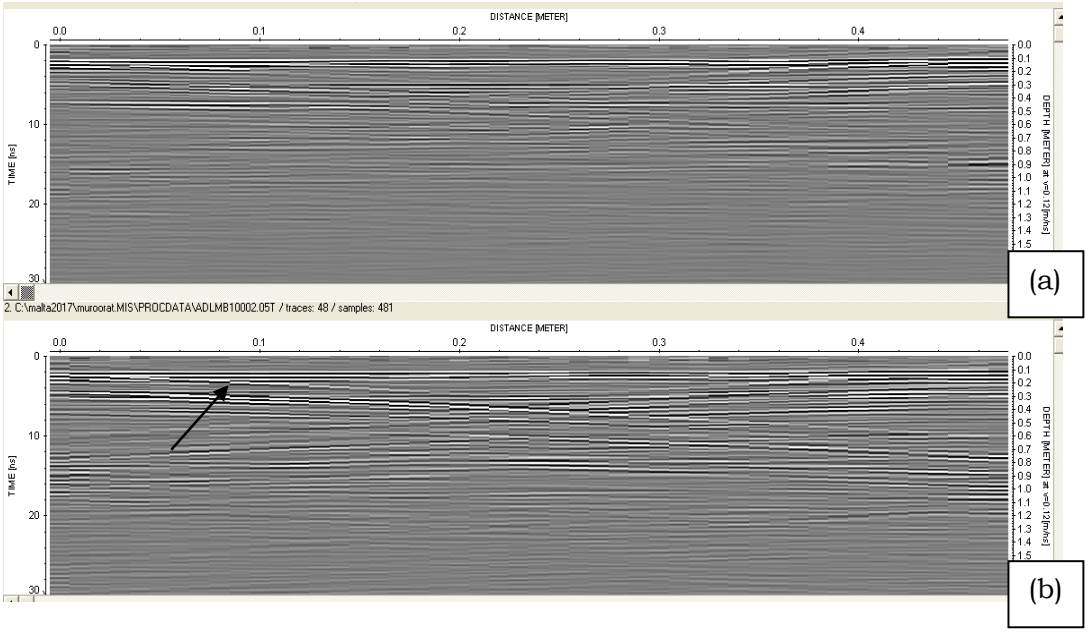

FIG. 20 - (a) B-Scan gathered on a 14-cm thick ashlar in the co-cathedral of St. John and (b) B-Scan gathered along the same path with a metallic sheet behind the ashlar.

We also performed a few more measurements on other walls, but the results were not clear, we therefore deem that they are not worth being presented.

5. GLOBIGERINA WALLS IN THE UNIVERSITY OF MALTA

Due to the poorness of the results achieved on the walls of the co-cathedral of St. John, we looked for a crossed comparison with some other structures. This was mainly done to verify whether the results obtained in the co-cathedral were reliable, and the walls of the co-cathedral can be really considered lossy and very dense (in an electromagnetic sense), or maybe there was an ill-functioning of the equipment or some trivial errors were done. We therefore decided to perform measurements on the walls of a building of the University of

https://doi.org/10.26376/GPR2018002

Malta, made of globigerina – which should be the same material composing the walls of the co-cathedral of St John.

In the University we achieved much clearer results, this confirmed that our equipment was working well and that our data acquisition method was correct. There probably just was a strong difference between the walls of the University and those of the co-cathedral. This may sound strange, because the walls are claimed to be made of the same material, and further studies are needed, in order to better understand the reasons of such differences. We can anticipate that preliminary waveguide measurements performed by the University of Malta on globigerina samples show that the relative permittivity of globigerina changes significantly when the water content varies. Moreover, even if the material of the University and co-cathedral walls were chemically the same, differences in the electromagnetic answer could be generated by a different porosity, which may be due to the different pressure level to which the two structures are subjected; finally, the different temperature in the two buildings may also have an effect (but this is expected to be a less influent factor).

One of the measurements was done at the first floor of department of physics of the University of Malta, on a 23-cm thick wall. The GPR system was the same IDS RIS HI Mode that was used in the co-cathedral, equipped with the same 2000 MHz antenna. Results are reported in Figure 21: in particular, in (a) we show the reflection generated by the other side of the wall (that in the case at hand was clearly visible), whereas in (b) three diffraction hyperbolas are matched. The processing was performed with the commercial software Reflexw. In Figure 21(b), a background removal was applied to the data in order to make more evident the (presumably) small reflectors that generated the diffraction hyperbolas. From Figure 21(a), we measured that the flat reflection occurred after 3.17 ns: with this timing and with formula (3), we estimated a propagation velocity in the wall of 14.51 cm/ns and a relative permittivity $\varepsilon_r = 4.27$.

Then, we put a copper sheet behind the wall and repeated the measurements. The results are presented in Figure 22. The presence of the metal sheet is made evident by the stronger reflection generated at the opposite side of the wall and also by the 'tail' occurring in the signal when the antenna passes beyond the maximum abscissa of the copper plate. Such tail is indicated by an arrow in Figure 22(a). In Figure 22(b)

https://doi.org/10.26376/GPR2018002

we repeated the measurements recorded without the metal sheet to facilitate the comparison.

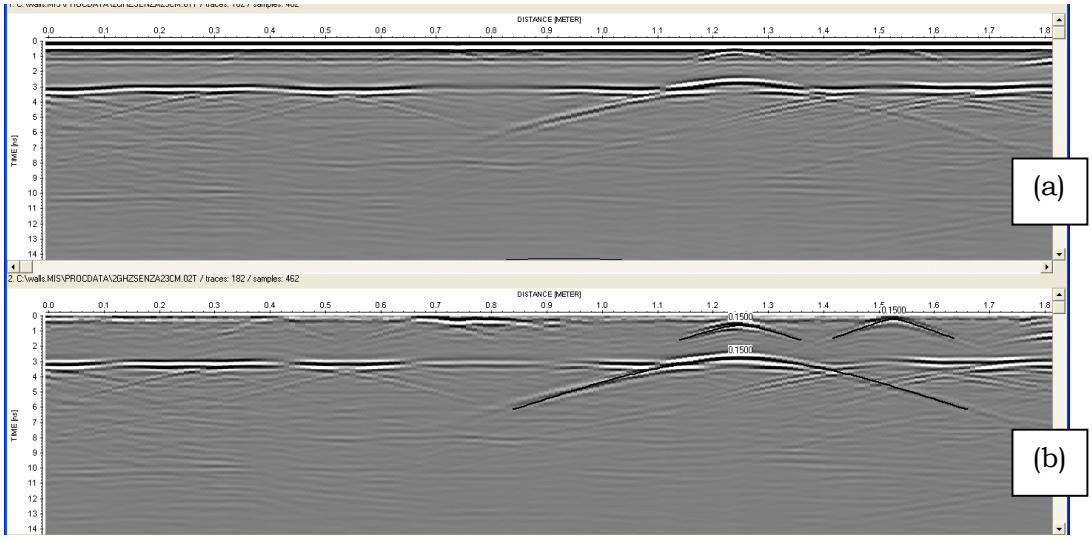

FIG. 21 - (a) GPR data recorded on a 23-cm thick wall, by using a 2000-MHz antenna; (b) the same signal as in (a), after background removal and with three diffraction hyperbolas matched.

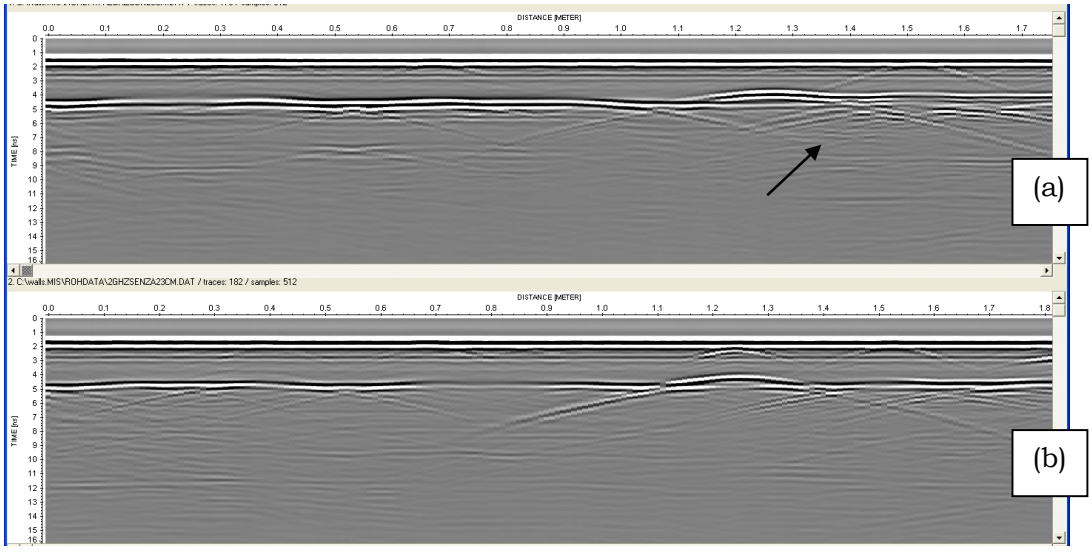

FIG. 22 - (a) Data recorded on the same wall as in Fig. 21, with a metal sheet behind the wall; (b) data recorded without the metal sheet, for comparison.

The same measurements, with and without metal sheet, were repeated by using an antenna with nominal central frequency at 900 MHz. The

https://doi.org/10.26376/GPR2018002

results are shown in Figure 23. The tail of the metal sheet is even more evident, but there is a loss of resolution that makes the antenna hardly suitable for the case at hand. In particular, in this case we cannot see evident diffraction hyperbolas reliably ascribable to small targets. From the return time of the flat reflector, we measured a return time of 3 ns and consequently a propagation velocity of 15.33 cm/ns and a relative permittivity $\varepsilon_r = 3.83$. The measurements at 2000 MHz look more reliable, because with the antenna at 900 MHz the resolution is of the same order as the return time.

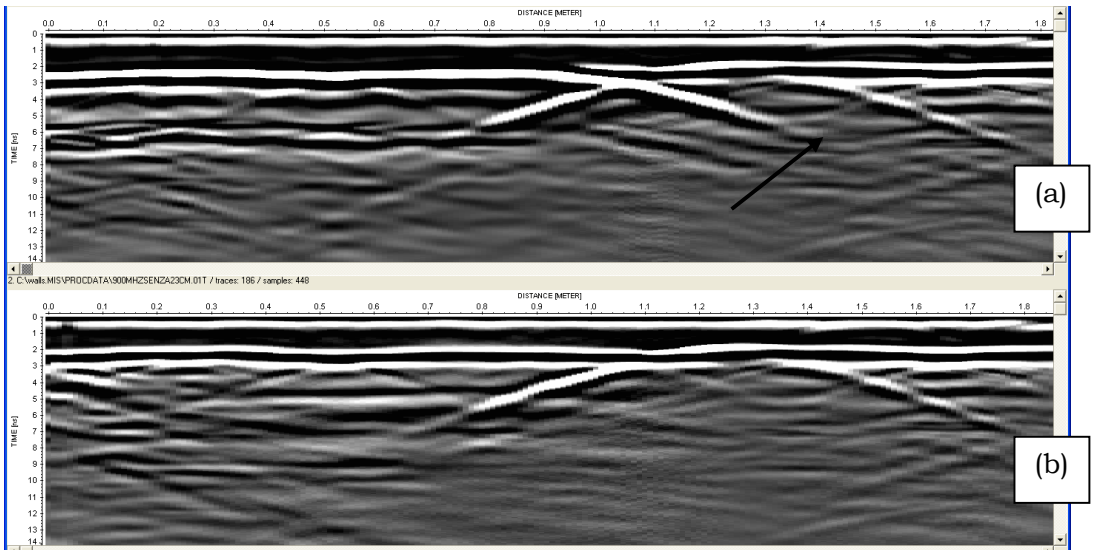

FIG. 23 - GPR data recorded on the same wall as in Fig. 21, by using a 900-MHz antenna, (a) with a metal sheet behind the wall and (b) without metal sheet. The arrow indicates the tail left by the metal sheet in the signal when the antenna went beyond it.

Then, we performed measurements on a wall at the ground floor of the same building, inside the department. This wall was 61 cm thick. Figure 24 shows the results obtained with the antenna at 900 MHz. In this case we measured a return time of 8 ns, corresponding to a propagation velocity of 15.25 cm/ns and to a dielectric permittivity $\varepsilon_r = 3.87$. We performed the measurements on the same wall also with the 2000-MHz antenna. The results are presented in Figure 25. It can be observed, both from Figure 25 and Figure 26, that the wall was not perfectly homogeneous. In particular, it contained three well visible anomalies, which may be related to internal reinforcement bars. From the data of Figure 25(a), we noticed that the reflection time from the

https://doi.org/10.26376/GPR2018002

most reflective point was t = 8.3 ns, yielding to a propagation velocity of 14.70 cm/ns and a relative permittivity ε_r = 4.17. From the radargram recorded without the sheet (Figure 25(b)) we retrieved t = 8.24 ns, with a propagation velocity of 14.81 cm/ns and a relative permittivity ε_r = 4.11.

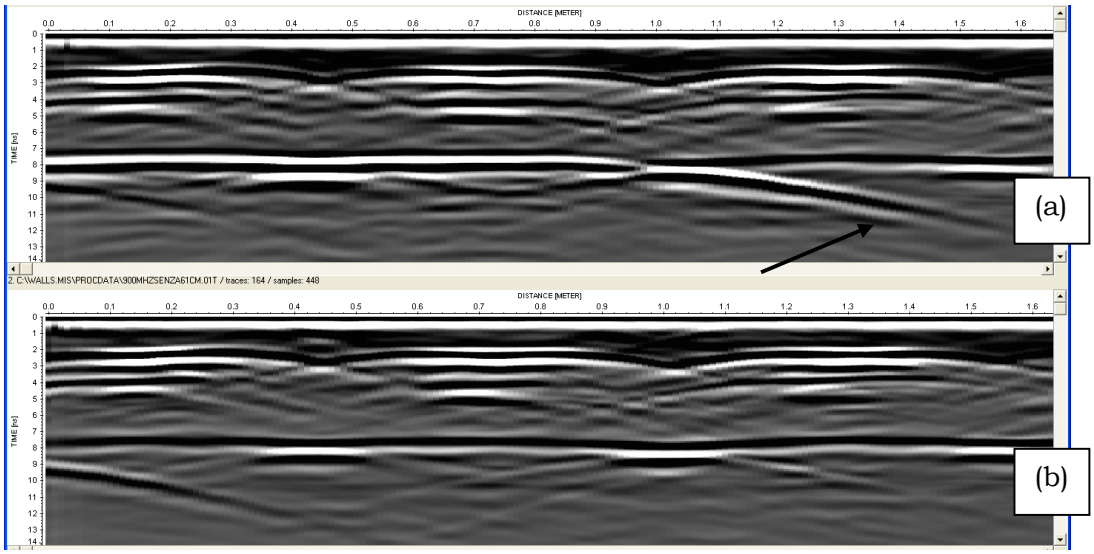

FIG. 24 – GPR data recorded on a 61-cm thick wall, with a 900-MHz antenna (a) with a metal sheet behind the wall, (b) without metal sheet. The arrow indicates the tail left by the metal sheet in the signal when the antenna went beyond it.

After that, we performed measurements on a pillar outside the department. The cross section of the pillar was a square, with an area of 45 × 45 cm^2. A first radargram was recorded on one side of the pillar, by using the 2000 MHz antenna (see Figure 26). The far side of the wall was hardly visible and the metal sheet did not leave any tail after its end. This indicated that the wall was probably more lossy than the walls inside the building, but we were not able to estimate the losses at this stage. In the data collected without metal sheet we observed two flattish reflections and this could generate ambiguity, whereas in the signal recorded with the metal sheet we observed only one flattish reflector, which masked the other one and made more reliable the relative-permittivity estimation. From these data, we measured t = 6.18 ns, a propagation velocity of 14.56 cm/ns and a relative permittivity ε_r = 4.24 without the metal sheet, and t = 6.3 ns, a propagation velocity of 14.29 cm/ns and a relative permittivity ε_r = 4.41 with the metal sheet.

https://doi.org/10.26376/GPR2018002

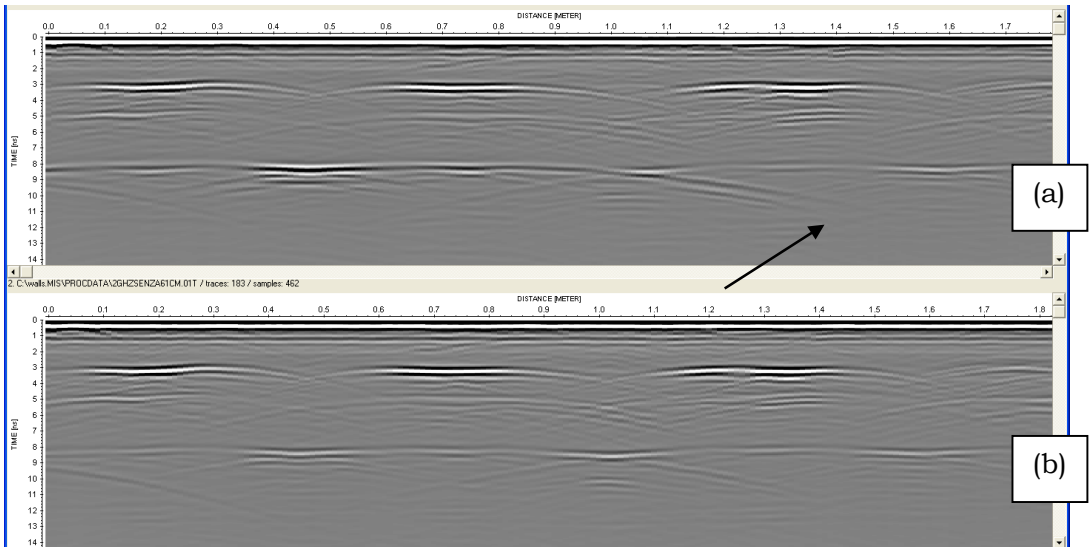

FIG. 25 - (a) GPR data recorded on a wall 61 cm thick with an antenna working at 2000 MHz and with a metal sheet behind the wall; (b) same as in (a), without the metal sheet. The arrow indicates the tail left by the metal sheet in the signal when the antenna went beyond it.

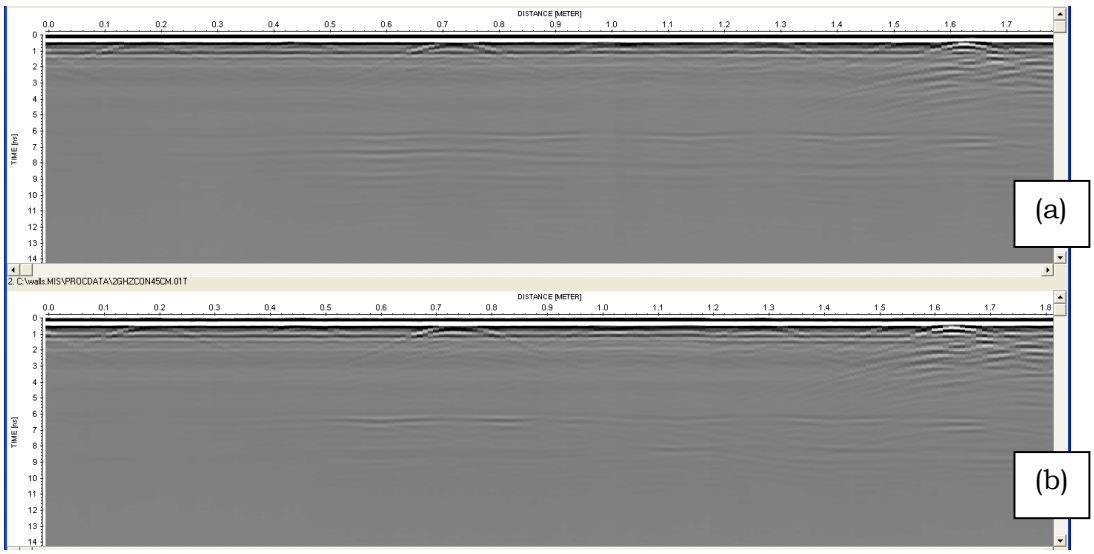

FIG. 26 - GPR data on a wall 45 cm thick, recorded with an antenna at 2000 MHz (a) without metal sheet behind the wall and (b) with the metal sheet.

We repeated the measurements with the same antenna on the two orthogonal sides of the same pillar. The results are presented in Figure 27. The data of Figure 27 are better than those of Figure 26, because

https://doi.org/10.26376/GPR2018002

the antennas were more centred with respect to the pillar, which was not possible in the previous case because of the presence of a railing. In Figure 27(b) we can observe (even if hardly) the tail of the metal sheet. The permittivity estimation did not change significantly, with respect to the estimation done on the basis of the results shown in Figure 26. This indicated that the material was not anisotropic, at least not along the cross plane.

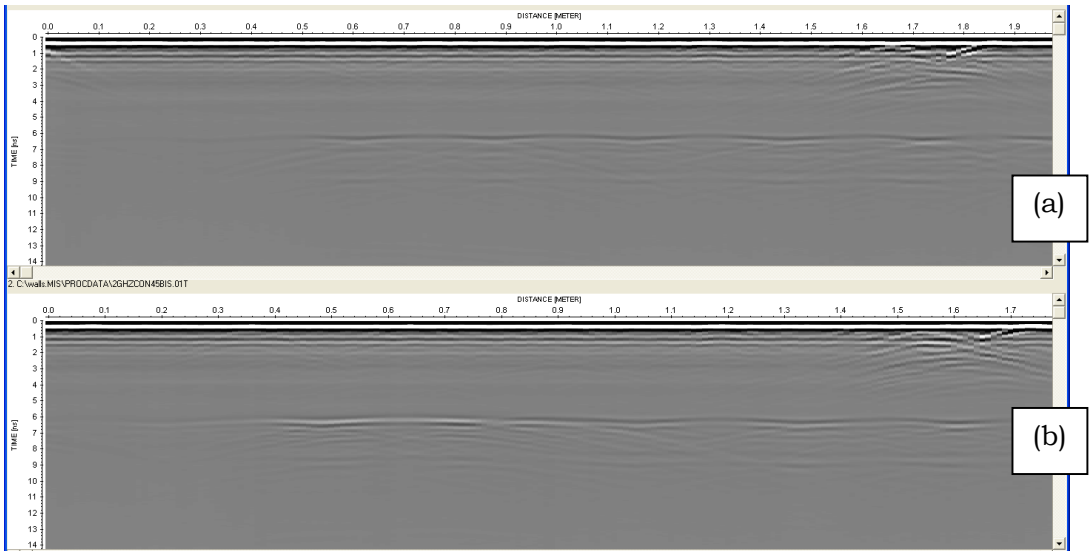

FIG. 27 – GPR data recorded on a wall 45 cm thick by using a 2000 MHz antenna, on the orthogonal sides of the pillar with respect to Figure 26, (a) without metal sheet behind the wall and (b) with the metal sheet.

Finally, we repeated the measurements on the same side of the pillar as in Fig. 27, but with the 900-MHz antenna. The recorded radargrams are presented in Figure 28. Now the metal sheet is well visible, because of the deeper penetration of the signal, and also the tail of the sheet is quite clear. The estimations based on the results in Figure 28 give: t = 6 ns, a propagation velocity of 15 cm/ns, and a relative permittivity $\varepsilon_r = 4$.

The discrepancies between the results achieved at 900 MHz and 2000 MHz may be partly ascribed to the frequency dispersion properties of the material. But mostly, they are ascribable to the worse resolution achievable with the 900 MHz antenna. The metal sheet might appear slightly longer or shorter in the various measurements: this is due to the fact that the odometer may slide without rotating in some cases, but this does not invalidate, of course, the achieved results.

https://doi.org/10.26376/GPR2018002

In conclusion, we considered three walls of different thickness made of the same material and found in different areas of the same University building, and the material turned out to be different in terms of electromagnetic properties.

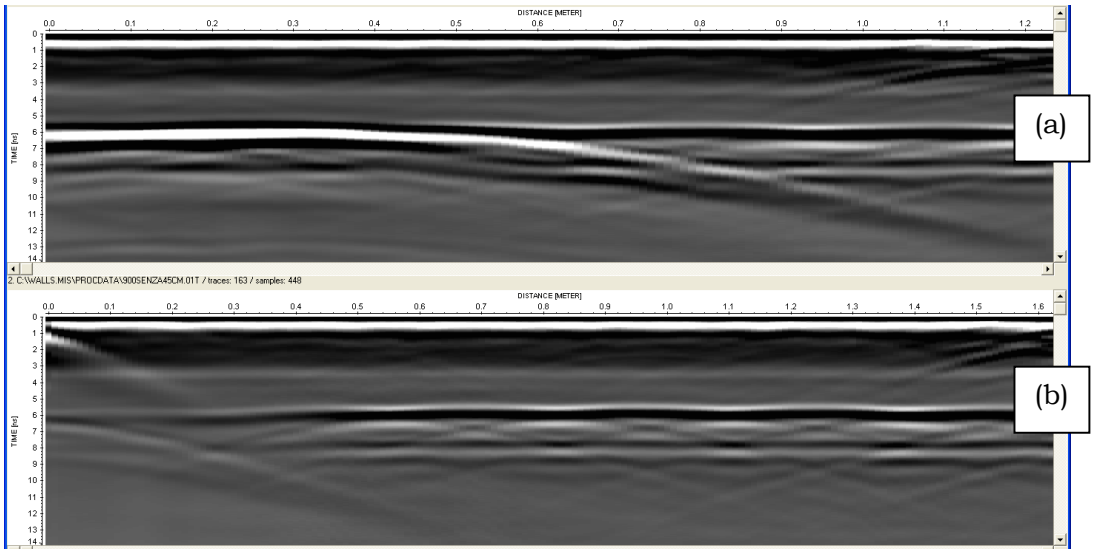

FIG. 28 – GPR data recorded on a wall 45 cm thick with an antenna at 900 MHz and (a) with a metal sheet behind the wall, (b) without metal sheet.

6. CONCLUSIONS

In this paper we presented the results of a series of Ground Penetrating Radar (GPR) surveys carried out in Malta, in sites of historical and cultural interest.

We first used a reconfigurable stepped-frequency GPR prototype to inspect the Argotti Garden in Floriana, looking for ancient buried cisterns, but we could not find them, mainly because we were authorised to gather just a limited number of profiles. Further investigations are needed and permission for gathering a grid of profiles is necessary, in order to get horizontal images of the ground, at different depths, which will help to discriminate whether some anomalies can be ascribable to the top of the sought cisterns. Moreover, and above all, we think that a three dimensional geoelectrical prospecting may provide better results, for this kind of investigation, than a GPR survey, given the depth and strong resistivity of the anomalies looked for.

https://doi.org/10.26376/GPR2018002

We then assessed the floor of the Nymphaeum inside the garden, to check its conditions prior to restoration works and verify whether cavities were present in the subsurface. We collected a grid of profiles by using our reconfigurable stepped-frequency GPR prototype. We found some anomalies close to the entrance of the Nymphaeum and excluded the presence of superficial cavities. We also observed that the floor of the Nymphaeum is made of a different material than the path leading to its entrance.

We subsequently used a commercial pulsed GPR system to assess the walls of the co-cathedral of St. John, in Valletta. The main purpose of our study was to detect internal fractures, meaningful gradients of moisture, or even possible structures inside the walls, hidden and walled during the past centuries. However, the walls turned out to be highly lossy and so the data that we recorded were obscure and difficult to be interpreted. We performed additional measurements on the walls of a building of the University of Malta, in Msida, which are made of the same material as the walls of the co-cathedral, for comparison. This allowed us to better understand the electromagnetic properties of the material at hand. We estimated the propagation velocity of the electromagnetic waves in the walls of the University building and their relative permittivity.

Acknowledgements

All measurements were performed during a Short-Term Scientific Mission (STSM) funded by the COST (European Cooperation in Science and Technology) Action TU1208 “Civil engineering applications of Ground Penetrating Radar.” Actually, the cooperation between the University of Malta and the Institute for Archaeological and Monumental Heritage of the National Research Council of Italy started in the framework of the COST Action TU1208, in July 2015, when a previous STSM was performed. The authors are grateful to COST for funding and supporting the Action TU1208.

References

[1] R. Persico and S. D’Amico, “Use of Ground Penetrating Radar and standard geophysical methods to explore the subsurface,” Ground Penetrating Radar, vol. 1(1), pp. 1-37, 2018.

https://doi.org/10.26376/GPR2018002

[2] R. Persico, D. Dei, F. Parrini, and L. Matera, Mitigation of narrow band interferences by means of a reconfigurable stepped frequency GPR system, Radio Science, pp. 1322–1331, 2016.

[3] R. Persico and G. Leucci, Interference Mitigation Achieved with a Reconfigurable Stepped Frequency GPR System, Remote Sensing, vol. 8(11), pp. 926–936, 2016.

[4] R. Persico, Introduction to Ground Penetrating Radar: Inverse Scattering and Data Processing, Wiley, 2014.

https://doi.org/10.26376/GPR2018002